J. Biochem. 119, 512-519 (1996)

^{13}C-NMR Study on the Interaction of Medium-Chain Acyl-CoA Dehydrogenase with Acetoacetyl-CoA[1]

Retsu Miura,*[,2] Yasuzo Nishina,† Shigeru Fujii,‡ and Kiyoshi Shiga†

*Departments of *Biochemistry and †Physiology, Kumamoto University School of Medicine, 2-2-1 Honjo, Kumamoto 960; and ‡Laboratory of Chemistry, Kansai Medical University, Hirakata, Osaka 573*

Received for publication, October 16, 1995

The charge-transfer interaction in the complex of pig kidney medium-chain acyl-CoA dehydrogenase (MCAD) with acetoacetyl-CoA was investigated by ^{13}C-NMR spectroscopy and molecular orbital treatment. The acyl carbons of acetoacetyl-CoA were separately ^{13}C-labeled and ^{13}C-NMR spectra of the complexes of MCAD with the ^{13}C-labeled acetoacetyl-CoA were measured. Each ^{13}C-carbon atom was observed as a distinct peak and easily distinguished from the protein background. The chemical shift values for free acetoacetyl-CoA were 198.5, 59.9, 208.8, and 32.8 ppm for C(1), C(2), C(3), and C(4), respectively, which shifted to 181.3, 103.4, 192.3, and 29.9 ppm, respectively, when acetoacetyl-CoA was complexed with MCAD. While C(4) underwent a small upfield shift, the other carbons experienced significant shifts; both the C(1) and C(3) carbonyl carbons shifted upfield by about 17 ppm, and the C(2) carbon was observed as a very broad peak at a position shifted downfield by more than 40 ppm. These results were compared with ^{13}C-NMR spectra of the keto-, enol-, and enolate forms of ethyl acetoacetate labeled with ^{13}C at the acyl carbons, and interpreted with reference to the charge-transfer model based on the optimum overlap between the lowest unoccupied molecular orbital (LUMO) of flavin and the highest occupied molecular orbital (HOMO) of the enolate state of the acetoacetyl moiety of acetoacetyl-CoA. The C(2) carbon of acetoacetyl-CoA takes on the sp^2 configuration in the bound form, indicating that one of the protons at C(2) of acetoacetyl-CoA is abstracted when bound to MCAD. C(1)=O is substantially polarized in the bound form of acetoacetyl-CoA, implying the presence of a machinery that polarizes this carbonyl group at the binding site, which thereby lowers the pK_a value of the α-proton at C(2). This machinery is of fundamental importance in the initial step of MCAD catalysis.

Key words: acetoacetyl-CoA, acyl-CoA dehydrogenase, ^{13}C-NMR, flavoenzyme, nuclear magnetic resonance.

Acyl-CoA dehydrogenase catalyzes the initial and rate determining step in the mitochondrial β-oxidation of fatty acids, which by this step undergo dehydrogenation to the corresponding *trans*-enoyl-CoA. The reductive half-reaction (dehydrogenation of substrate and reduction of flavin) proceeds *via* the concerted abstraction of the pro-*R*-α-proton from the substrate acyl-CoA by a protein base, Glu 376, in the case of medium-chain acyl-CoA dehydrogenase (MCAD), and the pro-*R*-β-hydride transfer to flavin (*1-3*). Several acyl-CoA dehydrogenases have been found to occur in mammalian mitochondria, and shown to have overlapping but distinct substrate specificities with respect to the chain length and structure of the acyl moiety. Among these enzymes, porcine MCAD, with high affinity to substrates with acyl-chain lengths of C6 to C10, has been most extensively studied by various physicochemical methods, including X-ray crystallography (*4*), and resonance Raman (*5*) and NMR (*6*) spectroscopy. Porcine MCAD is a homotetrameric flavoenzyme with FAD bound noncovalently to each subunit of the molecular mass of 42 kDa (*1*).

Flavoenzymes are known to form charge-transfer complexes with various ligands, including substrate analogs and competitive inhibitors, and more importantly with reaction intermediates during catalytic cycles. The charge-transfer interactions observed during flavoenzyme catalysis have mechanistic implications at critical stages (*7*). Acyl-CoA dehydrogenases, including MCAD, form a complex with acetoacetyl-CoA (AAC) characterized by a broad absorption band extending beyond 600 nm (Fig. 1). This complex has been postulated to be a charge-transfer complex involving the enolate anion of AAC (*7-10*), and this was proved by resonance Raman spectroscopy with excitation in the charge-transfer band (*5*). AAC, a competitive inhibitor of MCAD, is categorized as a 3-ketoacyl-CoA, which is not only a substrate analog for acyl-CoA dehydrogenases but also a product of an enzyme, 3-hydroxyacyl-CoA dehydrogenase, catalyzing a process a few steps away along the

[1] This study was supported in part by a Grant-in-Aid for Scientific Research from the Ministry of Education, Science and Culture of Japan.

[2] To whom correspondence should be addressed. Phone: +81-96-373-5062, Fax: +81-96-372-6140, E-mail: miura@gpo.kumamoto-u.ac.jp

Abbreviations: AAC, acetoacetyl-CoA; HOMO, highest occupied molecular orbital; LUMO, lowest unoccupied molecular orbital; MCAD, medium-chain acyl-CoA dehydrogenase.

β-oxidation pathway from the initial acyl-CoA dehydrogenation.

In the present study, we investigated the interaction of AAC with porcine MCAD at a submolecular level to gain a more precise insight into the fate of the substrate with respect to the reaction mechanism of the enzyme. The methods employed included purely theoretical treatment of molecular orbital calculation and experimental treatment utilizing ^{13}C-NMR spectroscopy. We have recently applied similar molecular orbital treatment to a flavoenzyme D-amino acid oxidase, and obtained essential information on the charge-transfer interactions with specific reference to the electron-transfer in both the reductive and oxidative half-reactions (*11*).

MATERIALS AND METHODS

Porcine kidney MCAD was purified as described previously by Gorelick *et al.* (*12*) and Lau *et al.* (*13*). The concentrations of MCAD and AAC were based on the molar extinction coefficients of 15.4 $mM^{-1} \cdot cm^{-1}$ at 446 nm (*14*) and 16 $mM^{-1} \cdot cm^{-1}$ at 260 nm (*15*), respectively.

^{13}C-labeled acetoacetyl-CoAs were prepared as described elsewhere (*16*). Ethyl [1,3-$^{13}C_2$]acetate (99 atom%), ethyl [2,4-$^{13}C_2$]acetate (99 atom%), and ethyl [3-^{13}C]acetoacetate (99 atom%) were purchased from Cambridge Isotope Laboratories. Other chemicals were of the highest grade available and used as supplied.

^{13}C-NMR spectra were measured in Wilmad 5-mm NMR tubes with a Varian UNITY 400 spectrometer operating at 100.6 MHz or with a Varian UNITY Plus 500 spectrometer operating at 125.7 MHz under proton irradiation. The flip angle was 50° for MCAD-AAC complexes with a relaxation delay time of 2 s, and 60° for free ethyl [^{13}C]acetoacetate with a relaxation delay time of 4 s. The NMR samples containing MCAD were in 50 mM potassium phosphate buffer, pH 6.0, at which the hydrolysis of AAC is negligibly slow during NMR measurements. All the NMR sample solutions contained 10% deuterium oxide for field locking. The ^{13}C-chemical shift was scaled in ppm downfield relative to the methyl carbon signal of external 3-(trimethylsilyl) propionate-d_4. The concentration of MCAD in NMR experiments was 0.7 mM. Some of the chemical shift values reported elsewhere were relative to tetramethylsilane. For comparison of such chemical shift values relative to tetramethylsilane with those in the present study, 1.6 ppm was added to each of the values referenced to tetramethylsilane (*6*). MCAD-AAC complexes for NMR measurement were prepared by adding a slight molar excess of lyophilized AAC powder to the MCAD solution, followed by standing for 30 min at room temperature prior to NMR measurement. On the basis of the dissociation constant of 12 μM for the MCAD-AAC complex (*17*), and the concentrations of MCAD and AAC, MCAD in the NMR samples was saturated with AAC. The ^{13}C-NMR spectra of ethyl [^{13}C]acetoacetate were measured at a concentration of 30 mM in either 1 M potassium phosphate, pH 7.4, or 1 N NaOH.

Extended Hückel molecular orbital calculations were performed with a program provided by Nishimoto *et al.* (*18*) run on an NEC PC9801-Vm personal computer. The principal molecular parameters used for 5-thiahexan-2,4-dione were: $r(C_1\text{-}C_2) = 1.53$ Å, $r(C_2\text{-}C_3) = 1.466$ Å, $r(C_3\text{-}C_4) = 1.36$ Å, $r(C_4\text{-}S_5) = r(S_5\text{-}C_6) = 1.81$ Å, r(C-H) = 1.07 Å, $\alpha(C_1C_2O) = \alpha(C_3C_2O) = \alpha(C_3C_4O) = \alpha(S_5C_4O) = 120°$, $\alpha(C_6S_5C_4) = 105°$.

RESULTS

Molecular Orbital Treatment of the Charge-Transfer Interaction between Anionic Acetoacetyl-CoA and Flavin— It has been demonstrated that AAC forms a charge-transfer complex with MCAD, as mentioned earlier (Fig. 1), and that AAC bound to MCAD is the deprotonated anionic form. As it was confirmed that the MCAD-AAC complex involves a charge-transfer interaction between oxidized flavin and the acyl-moiety of AAC (*5*), we evaluated the overlap between the molecular orbitals of flavin and AAC. Since the flavin moiety in MCAD accepts electrons from substrate acyl-CoA, oxidized flavin serves as the charge acceptor and AAC as the charge donor. Therefore we calculated the highest occupied molecular orbital (HOMO) of the enolate anion of 5-thiahexan-2,4-dione, a model compound for anionic acetoacetyl-CoA, by the extended Hückel molecular orbital method, and aligned it with the lowest unoccupied molecular orbital (LUMO) of oxidized flavin reported by Nishimoto *et al.* (*19*). Since the acetoacetyl portion in the enolate form is planar, there are four possible conformations for the enolate anion of the model compound. Figure 2 represents the HOMO of the model compound in the particular conformation that overlaps best with the flavin LUMO with respect to both the magnitude of overlap and the symmetric arrangements of atomic orbitals. Note that the maximum overlap was observed between orbitals corresponding to C(2) of acetoacetyl-CoA and N(5) of the flavin nucleus. This is in accordance with the specific ^{15}N-chemical shift change of flavin N(5) in the MCAD-AAC complex (*6*), and agrees with the resonance Raman results showing that the C(4*a*)=N(5) moiety of flavin participates in the charge-transfer interaction with acetoacetyl-CoA while the dimethylbenzene moiety does not (*5, 16*). The resonance Raman studies (*5, 16*) were performed with excitation at 632.8 nm, which is within the

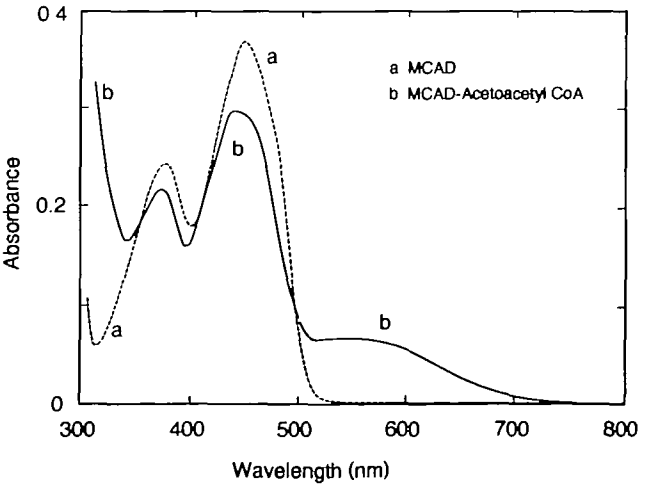

Fig. 1. **Absorption spectra of medium-chain acyl-CoA dehydrogenase (MCAD) and its complex with acetoacetyl-CoA.** Spectra were measured in 50 mM potassium phosphate, pH 7.6. The concentrations were: MCAD, 23.7 μM (a) and 23.2 mM (b); acetoacetyl-CoA, 135 μM.

charge-transfer band (Fig. 1).

^{13}C-NMR of the MCAD-AAC Complex—^{13}C-NMR spectra of the complexes of MCAD with AAC labeled with ^{13}C at carbonyl carbons C(1) and C(3) are shown in Fig. 3. The peaks of each ^{13}C-labeled carbon for the free and MCAD-bound forms were clearly discernible, as indicated in the figure. Though the ^{13}C(1) signal for the MCAD-bound state is conspicuous when the two spectra taken at 100.6 MHz in Fig. 3 are compared, the signal is within the protein background peak. For confirmation of the ^{13}C(1) resonance peak, a ^{13}C-NMR spectrum of the same sample was measured at 125.7 MHz. The signal was confirmed, as shown in the inset. Both the carbonyl carbons exhibited a large upfield shift by about 17 ppm when AAC was bound to MCAD (Table I).

Figure 4 shows the ^{13}C-NMR spectra of the complexes of MCAD with AAC labeled with ^{13}C at the methylene C(2) and methyl C(4) carbons. While the methyl ^{13}C(4) signal marked a slight upfield shift by about 3 ppm, the methylene ^{13}C(2) signal was observed at a remarkably lower field, by 44 ppm, as a very broad peak, the half width being approximately 160 Hz. This exceptional width may reflect the specific nature of the C(2) position in the interaction with flavin and may be relevant as to the great overlap of the atomic orbital at this position with the flavin N(5) atomic orbital, as described in the preceding section. The chemical shift values for the individual carbons are summarized in Table I.

^{13}C-NMR of Ethyl [^{13}C]Acetoacetate—In order to better interpret the chemical shift differences of AAC in the free and MCAD-bound forms, we measured ^{13}C-NMR spectra of ethyl acetoacetate labeled with ^{13}C at the acyl carbons at pH 7.4 and in 1 N NaOH (Figs. 5 and 6). The assignments for the ^{13}C(1) and ^{13}C(3) resonance peaks shown in Fig. 5 were confirmed by comparison with the spectra of ethyl [3-^{13}C]-acetate at pH 7.4 and in 1 N NaOH (data not shown). The ^{13}C(2) and ^{13}C(4) resonance peaks shown in Fig. 6 are within the regions expected for methyl and methylene carbons, respectively, and are assigned as such in the upper spectrum. The signals expected for methyl resonance in the lower spectrum were assigned as C(4) and thereby the other peak was assigned as C(2). The thioester bond in acyl-CoA is not stable in alkali, and acetoacetyl-CoA is rapidly hydrolyzed to acetoacetate and CoA-SH in an NaOH solution; therefore, the observation of ^{13}C-signals for anionic acetoacetyl-CoA was not possible. In fact, even ethyl acetoacetate was hydrolyzed in 1 N NaOH at 20°C, at which NMR spectra were taken, with a half life of about 30 min, as observed during NMR measurement; Fig. 6 shows the presence of hydrolyzed species, acetoacetate (asterisks in the lower trace), even a few minutes after the mixing of ethyl acetoacetate with 1 N NaOH. Ethyl acetoacetate in 1 N NaOH is in the anionic form, since the pK_a value of the methylene proton at C(2) is 10.7 (*20*). The chemical shift values are summarized in Table II, which also contains those in chloroform of the keto and enol forms (*21*) for comparison. Two sets of chemical shifts were observed at pH 7.4 and in 1 N NaOH. This can be ascribed to different conformations, the details of which were not pursued here since the conclusions obtained below are not specifically dependent on the conformational differences.

Though the enol form of ethyl acetoacetate can assume two tautomeric forms (Scheme 1(1); II and III), the tautomer (II) predominates in chloroform (*21*), in which a C=O double bond preferentially occurs at C(1) rather than C(3). This conclusion is based on the chemical shift differences of C(1) and C(3) between the keto and enol forms; C(1) shifts moderately downfield when going from the keto to the enol form, whereas C(3) shifts considerably upfield by about 30 ppm (lower two rows in Table II). The most prominent difference between the keto and enol forms is seen in C(2); C(2) of the enol form is at 40 ppm downfield from that of the keto form (lower two rows in Table II). This change is well within the range expected from the hybridization dependence on the ^{13}C-chemical shift (*22*). The hybridization of C(2) of the keto form (I) is sp^3, whereas that of the enol form (II/III) is sp^2. The latter hybridization gives a low-field resonance position compared to the former (*22*).

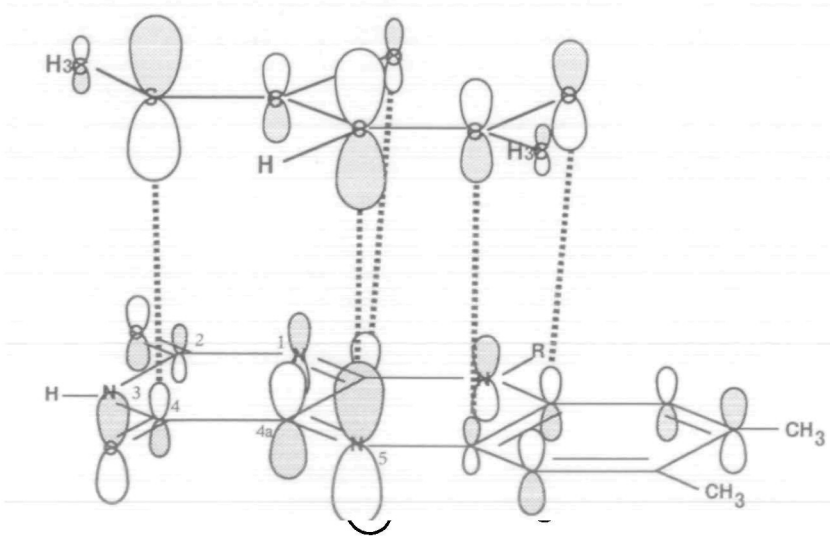

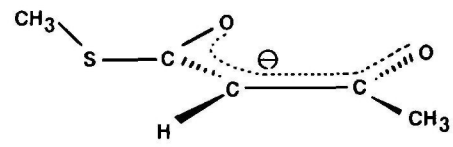

5-Thiahexan-2,4-dione (anionic)

Fig. 2. **Optimum overlap between LUMO of lumiflavin (R=CH$_3$) (*13*) and HOMO of the enolate form of 5-thiahexan-2,4-dione.** Out of the four possible conformations for 5-thiahexan-2,4-dione enolate, the one with the best overlap in terms of magnitude and symmetry is presented.

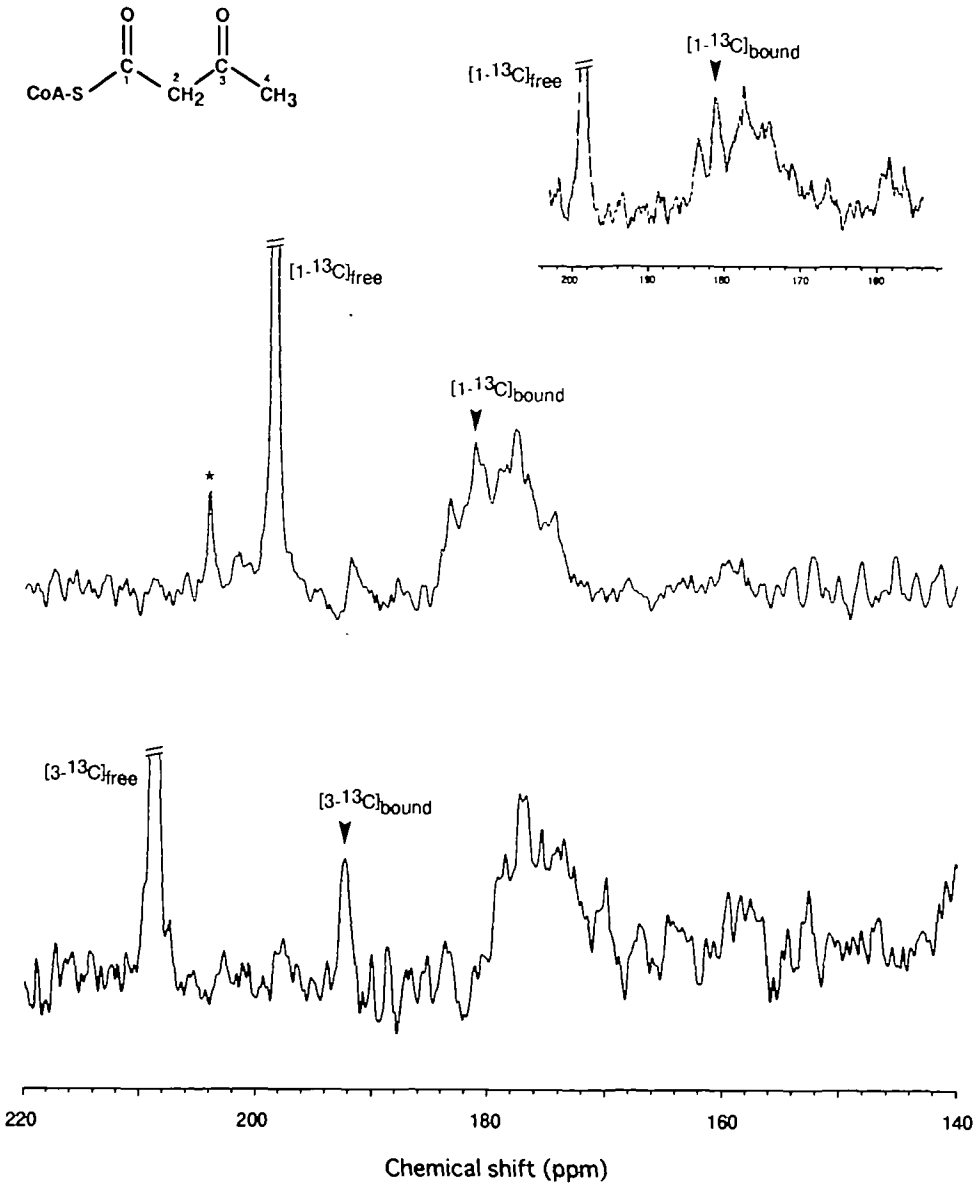

Fig. 3. **^{13}C-NMR spectra of the complexes of MCAD with [1-^{13}C] acetoacetyl-CoA (upper trace) and [3-^{13}C]acetoacetyl-CoA (lower trace).** The observation frequency was 100.6 MHz. The numbers of scans were 25,000 (upper) and 12,000 (lower). The inset shows the spectrum of [1-^{13}C]acetoacetyl-CoA·MCAD with the observation frequency of 125.7 MHz under similar conditions. A window function corresponding to 40 Hz was applied to each spectrum. The peak denoted by an asterisk is due to the minor amount of acetoacetate as the result of hydrolysis of acetoacetyl-CoA.

TABLE I. **^{13}C-chemical shifts of ^{13}C-labeled acetoacetyl-CoA free and bound to medium-chain acyl-CoA dehydrogenase.**

	Positions			
	1	2	3	4
Free	198.5	59.9	208.8	32.8
MCAD-bound	181.3	103.4	192.3	29.9
Bound-free	−17.2	+43.5	−16.5	−2.9

The chemical shift values for ethyl acetoacetate at pH 7.4 parallel those of the keto-form in chloroform, indicating that ethyl acetoacetate exists as its keto form (Scheme 1(1); I) in a neutral aqueous medium. In 1 N NaOH, ethyl acetoacetate is in its anionic form, as described above. Though three tautomeric forms are possible for the anionic ethyl acetoacetate (Scheme 1(2); IV-VI), enolate forms (V and VI) are expected to predominate due to the extended conjugation. This agrees with the chemical shift of C(2), which was observed in the sp^2 carbon region at a lower field by about 35 ppm (Table II, upper two rows). Furthermore, though C(1) of the anionic form was observed at a slightly lower field compared to that of the keto form at pH 7.4, C(3) experienced an upfield shift of about 20 ppm when going from the keto to the enolate form (Table II, upper two rows). These results indicate clearly that the enolate form of ethyl acetoacetate is predominantly in the tautomeric form (V), where the CO bond at C(1) is a double bond and that at C(3) is a single bond. On the basis of the above interpretation, the following three conclusions can be drawn from Table II. (i) C(1) of ethyl acetoacetate links oxygen preferentially in a double bond whether ethyl acetoacetate is in the enol or enolate form, and C(3) links oxygen in a single bond in either the enol or enolate form. (ii) When a carbonyl carbon becomes an enol or enolate carbon, as in C(3) of ethyl acetoacetate (II or V), the ^{13}C-chemical shift decreases by 20-30 ppm. (iii) When the sp^3 C(2) carbon in the 1,3-diketone system of ethyl acetoacetate takes the sp^2 hybridization as the result of enoliza-

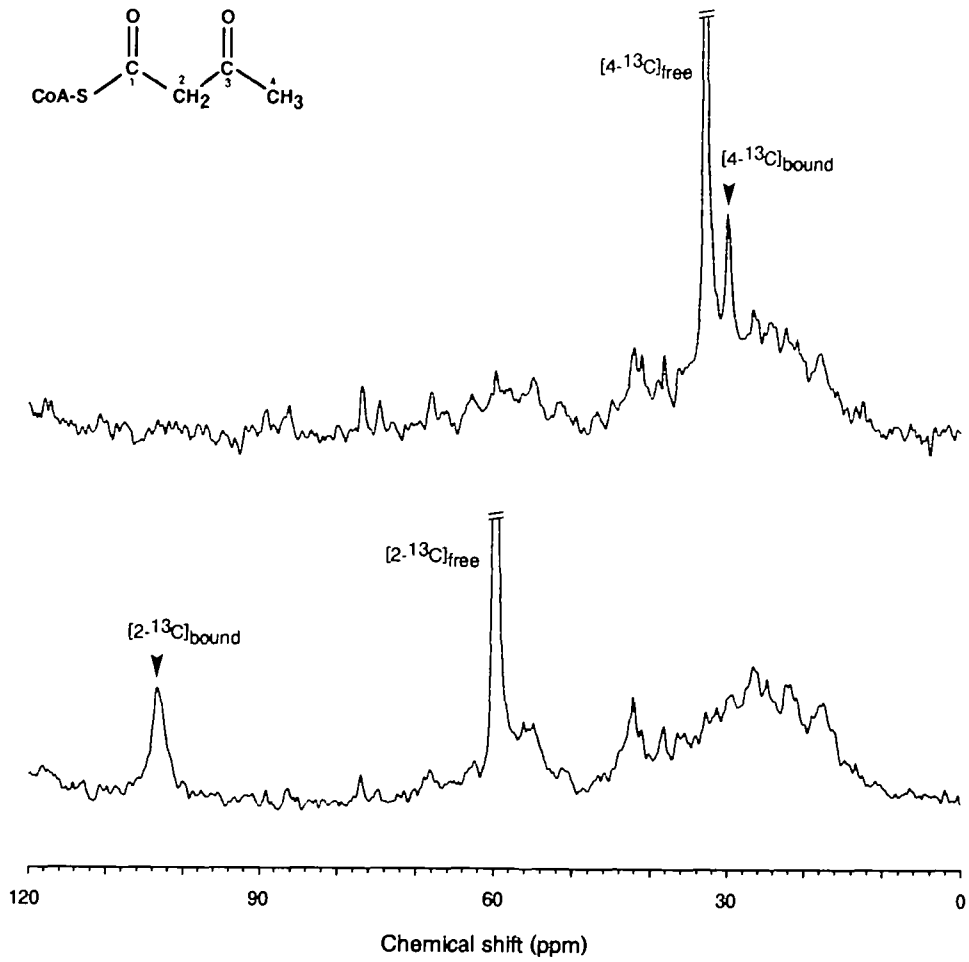

Fig. 4. **^{13}C-NMR spectra of the complexes of MCAD with [4-^{13}C]-acetoacetyl-CoA (upper trace) and [2-^{13}C]acetoacetyl-CoA (lower trace).** The observation frequency was 100.6 MHz. The numbers of scans were 6,500 (upper) and 25,000 (lower). A window function corresponding to 40 Hz was applied to each spectrum.

tion or enolate anion formation, the carbon undergoes a downfield shift by 30-40 ppm.

DISCUSSION

The charge-transfer complex model for MCAD-AAC, as deduced on molecular orbital treatment (Fig. 2), exhibits a maximum overlap at flavin N(5) and thus explains the specific interactions at N(5) of the flavin ring system manifested in the large ^{15}N-chemical shift change when MCAD forms a complex with AAC (*6*). The mutual orientation between flavin and the ligand in Fig. 2 enables the interaction of C(1)=O of the substrate with the ribityl side chain of FAD; the crystal structure of the MCAD•octanoyl-CoA complex exhibits a hydrogen-bonding interaction between C(1)=O and 2′-OH of the ribityl side chain of FAD (*4*). The extensive overlap between the C(2) atomic orbital of the AAC model and that of flavin N(5) may constitute the basis for the markedly broad signal of the C(2) of AAC when bound to MCAD (Fig. 3). The line width of the resonance signal for ^{13}C(2) of the enol or enolate form of ethyl acetoacetate is within the normal line width range (*21* and Fig. 6). There may be a unique relaxation mechanism through the overlapping orbitals, resulting in a shorter relaxation time responsible for a broad peak. Alternatively, some yet unknown exchange phenomena may have resulted in the unusual line width.

Ethyl acetoacetate represents a good model for AAC, since both compounds have the acetoacetyl portion in common, and the sulfur atom in AAC is replaced by a homologous oxygen in ethyl acetoacetate, making it more durable in an alkaline medium, so that its enolate anion can be analyzed by NMR. Comparison of the chemical shift values of free AAC in Table I with those of ethyl acetoacetate at neutral pH (Table II) clearly demonstrates that the free AAC is in the keto form (Scheme 1(3); VII). Though the chemical shift values of C(3) in the keto forms of AAC and ethyl acetoacetate in aqueous solution agree well with each other, C(1) for AAC was observed at a lower field by 26 ppm (first rows in Tables I and II). This difference should be found in the ethoxy oxygen in ethyl acetoacetate in place of the sulfur atom in AAC at the corresponding position. The *n*-orbital for the lone pair electrons of the ethoxy oxygen can overlap with the *p*-orbital of C(1)=O, endowing a fractional single bond character on the C(1)=O double bond. This manifests itself in the relatively high field position (172.4 ppm) of the C(1) carbonyl carbon of ethyl acetoacetate. In contrast, the overlap of the sulfur *n*-orbital with the carbonyl π-orbital is less extensive because the sulfur *n*-orbital utilizes the 3*p*-orbital and the carbonyl π-orbital uses the 2*p*-orbital, hence more double bond character of the thioester carbonyl explaining the lower field position (198.5 ppm) for C(1) of free AAC than that for C(1) of ethyl acetoacetate.

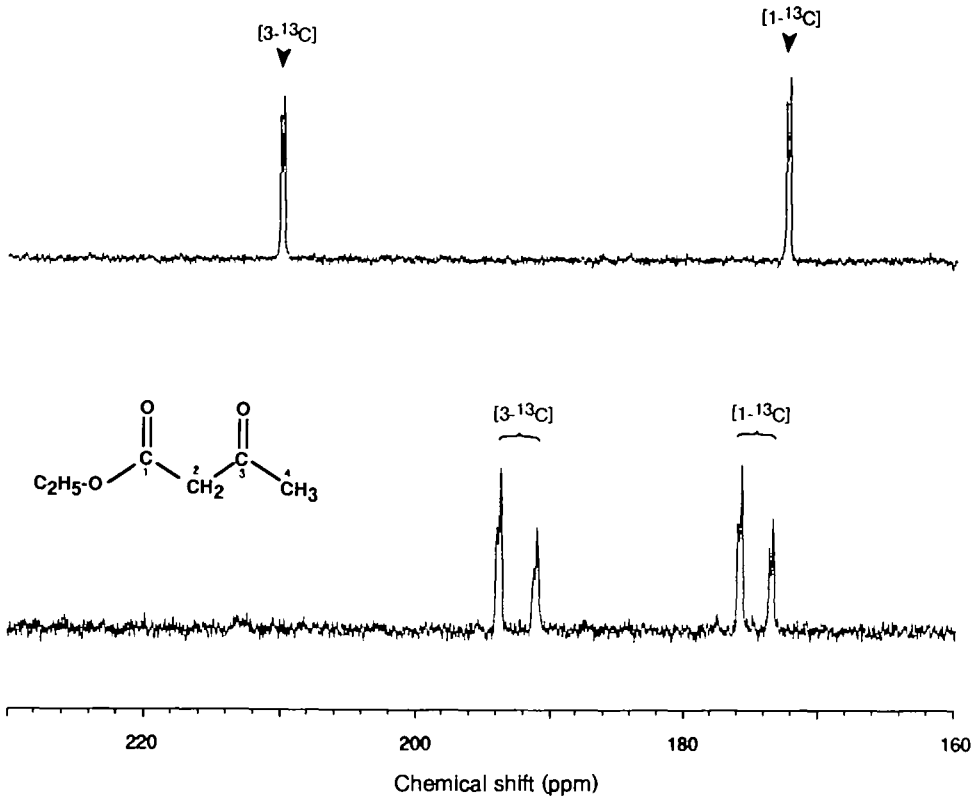

Fig. 5. **^{13}C-NMR spectra of ethyl [1,3-$^{13}C_2$]acetoacetate in 1 M potassium phosphate, pH 7.4 (upper trace), and 1 N NaOH (lower trace).** The number of scans was 32. The observation frequency was 125.7 MHz. A window function corresponding to line-broadening of 4 Hz was applied to each spectrum. The lower spectrum was taken immediately after mixing the compound with 1 N NaOH.

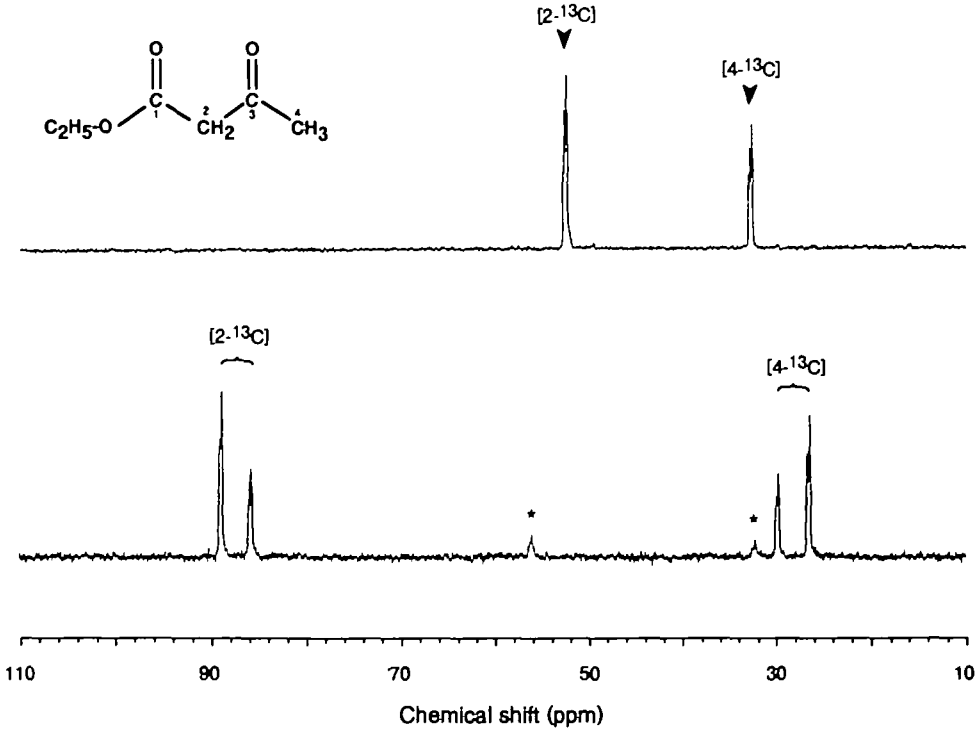

Fig. 6. **^{13}C-NMR spectra of ethyl [2,4-$^{13}C_2$]acetoacetate in 1 M potassium phosphate, pH 7.4 (upper trace), and 1 N NaOH (lower trace).** The number of scans was 32. The observation frequency was 125.7 MHz. A window function corresponding to line-broadening of 4 Hz was applied to each spectrum. The lower spectrum was taken immediately after mixing the compound with 1 N NaOH. The asterisks indicate the peaks of the hydrolyzed species, acetoacetate (see the text).

The resonance position of ^{13}C(2) of AAC in the MCAD-bound form was observed at a lower field from that of free AAC by 43.5 ppm indicating that C(2) of AAC bound to MCAD undergoes sp^2 hybridization. This is in accordance with the notion that AAC complexed with MCAD takes on the anionic enolate form (*7-10*). The change in the hybridization of C(2) from sp^3 to sp^2 when bound to MCAD requires labilization of the α-proton at the active site, the prerequisite process in the reductive half-reaction of MCAD. Equally important are the patterns of the chemical

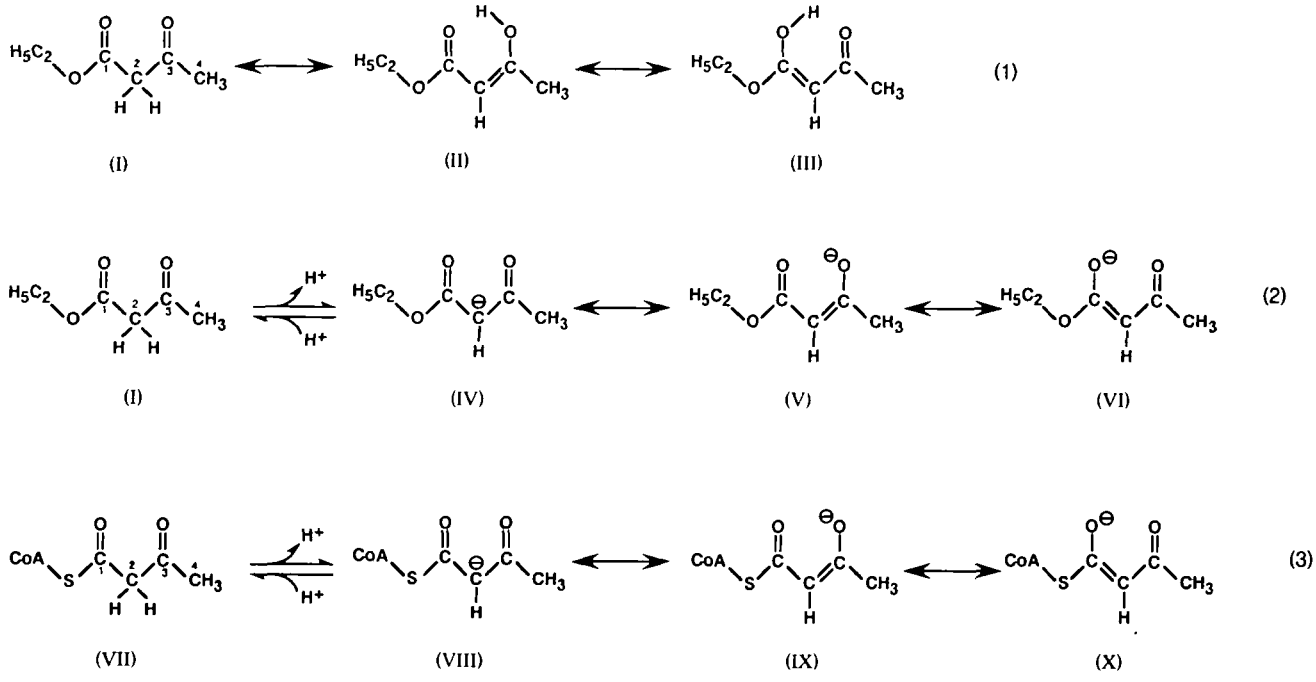

Scheme 1

TABLE II. ^{13}C-chemical shifts of the acetoacetyl portion of ethyl acetoacetate.

	Positions			
	1	2	3	4
pH 7.4 (Keto form)	172.4	52.5	209.8	32.9
		52.2		32.5
1 N NaOH (Enolate)	175.9	88.8	193.7	29.8
	173.6	85.6	191.0	26.6
Keto form[a] (Chloroform)	170.4	52.1	203.9	31.7
Enol form[a] (Chloroform)	179.1	92.1	175.9	22.7

[a]Values taken from Breitmaier and Voelter (*21*).

shift changes of carbonyl carbons C(1) and C(3), particularly that of C(1). Both ^{13}C(1) and ^{13}C(3) shifted upfield by about 17 ppm. We should be reminded by the model studies with ethyl acetoacetate that the C(1) carbonyl retains its double bond character when AAC is in the enol or enolate form in an aqueous medium, while the C(3) carbonyl preferentially becomes an enol(ate) single bond. This would predict a slight downfield shift for C(1) and a considerable upfield shift of 20–30 ppm for C(2) if AAC bound to MCAD takes on the electronic state expected from the model study for free ethyl acetoacetate. Both C(1) and C(3) of AAC exhibited similar upfield shifts of about 17 ppm when bound to MCAD, indicating similar degrees of a single bond character for C(1)O and C(3)O bonds. The experimental observations are in clear contrast to the expected behaviors of these carbons. The upfield shift of C(1) for the bound AAC provides explicit evidence that the C(1) carbonyl is substantially polarized in the MCAD-bound state compared to that free in an aqueous solution, where polarization of C(1)=O is slight, if any, as expected from the model study. Namely, the tautomerization equation for enolate of AAC (Scheme 1(3); IX and X) is shifted considerably to X in the MCAD-bound state compared to the free form in an aqueous environment. There exists, therefore, a machinery

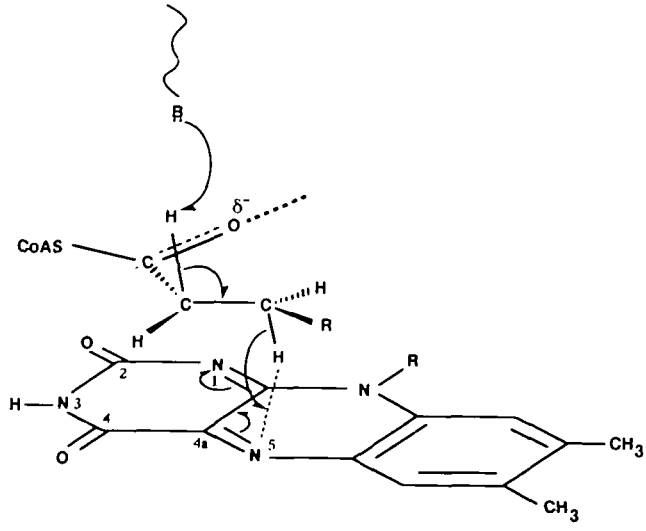

Fig. 7. **Reductive half-reaction of MCAD.** The thick dotted line represents the machinery for polarizing C(1)=O. The degree of polarization is indicated by δ^-. The orientation of the substrate with respect to the flavin system takes into account the HOMO-LUMO interaction in Fig. 2.

in the acyl-CoA binding site of MCAD that polarizes the C(1)=O carbonyl group. This polarizing machinery should act on C(1)=O of the substrate acyl-CoA and polarize the carbonyl group, thereby lowering the pK_a of the α-proton and thus making the β-hydride-transfer more feasible (Fig. 7). The polarizing effect in question is one of the focuses for understanding the molecular mechanism underlying the substrate activation (*4, 23, 24*). We have shown here that the behavior of the ^{13}C(1) signal constitutes a unique and direct means of evaluating the polarizing effect.

The shift in the tautomerization of enolate of AAC

toward X in Scheme 1(3) when AAC is bound to MCAD was suggested by our previous resonance Raman studies (*5*). The present results reinforce the conclusion drawn from the resonance Raman experiments and provided compensatory information for evaluating the polarization of C(1)=O of the substrate. The chemical shift behavior of C(1)=O should be explored with other acyl-CoA dehydrogenases, using 3-ketoacyl-CoA with different acyl-chain lengths or with different acyl structures. Experiments along these lines are currently in progress.

REFERENCES

1. Engel, P.C. (1992) Acyl-coenzyme A dehydrogenases in *Chemistry and Biochemistry of Flavoenzymes* (Müller, F., ed.) Vol. III, pp. 597-655, CRC Press, Boca Raton, Ann Arbor, London
2. Ghisla, S., Vock, S.E.P., Kieweg, V., Bross, P., Nandy, A., Rasched, I., and Strauss, A.W. (1994) Mechanisms of α,β-dehydrogenation by acyl-CoA dehydrogenases in *Flavins and Flavoproteins 1993* (Yagi, K., ed.) pp. 283-292, Walter de Gruyter, Berlin, New York
3. Thorpe, C. and Kim, J.-J.P. (1995) Structure and mechanism of action of the acyl-CoA dehydrogenases. *FASEB J.* **9**, 718-725
4. Kim, J.-J.P., Wang, M., and Paschke, R. (1993) Crystal structures of medium-chain acyl-CoA dehydrogenase from pig liver mitochondria with and without substrate. *Proc. Natl. Acad. Sci. USA* **90**, 7523-7527
5. Nishina, Y., Sato, K., Shiga, K., Fujii, S., Kuroda, K., and Miura, R. (1992) Resonance Raman study on complexes of medium-chain acyl-CoA dehydrogenase. *J. Biochem.* **111**, 699-706
6. Miura, R., Nishina, Y., Sato, K., Fujii, S., Kuroda, K., and Shiga, K. (1993) ^{13}C- and ^{15}N-NMR studies on medium-chain acyl-CoA dehydrogenase reconstituted with ^{13}C- and ^{15}N-enriched flavin adenine dinucleotide. *J. Biochem.* **113**, 106-113
7. Massey, V. and Ghisla, S. (1974) Role of charge-transfer interactions in flavoprotein catalysis. *Ann. N.Y. Acad. Sci.* **227**, 446-465
8. Engel, P.C. and Massey, V. (1971) Green butyryl-coenzyme A dehydrogenase. An enzyme-acyl-coenzyme A complex. *Biochem. J.* **125**, 889-902
9. McKean, M., Frerman, F.E., and Mielke, D.M. (1979) General acyl-CoA dehydrogenase from pig liver. Kinetic and binding studies. *J. Biol. Chem.* **254**, 2730-2735
10. Thorpe, C. and Massey, V. (1983) Flavin analogue studies of pig kidney general acyl-CoA dehydrogenase. *Biochemistry* **22**, 2972-2978
11. Nishina, Y., Sato, K., Miura, R., and Shiga, K. (1995) Structure of charge-transfer complexes of flavoenzyme D-amino acid oxidase: A study by resonance Raman spectroscopy and extended Hückel molecular orbital method. *J. Biochem.* **118**, 614-620
12. Gorelick, R.J., Mizzer, J.P., and Thorpe, C. (1982) Purification and properties of electron-transferring flavoprotein from pig kidney. *Biochemistry* **21**, 6936-6942
13. Lau, S.-M., Powell, P., Buettner, H., Ghisla, S., and Thorpe, C. (1986) Medium-chain acyl coenzyme A dehydrogenase from pig kidney has intrinsic enoyl coenzyme A hydratase activity. *Biochemistry* **25**, 4186-4189
14. Thorpe, C., Matthews, R.G., and Williams, C.H., Jr. (1979) Acyl-coenzyme A dehydrogenase from pig kidney. Purification and properties. *Biochemistry* **18**, 331-337
15. Stadtman, E.R. (1957) Preparation and assay of acyl coenzyme A and other thiol esters: Use of hydroxylamine in *Methods in Enzymology* (Colowick, S.P. and Kaplan, N.O., eds.) Vol. 3, pp. 931-941, Academic Press, New York
16. Hazekawa, I., Nishina, Y., Sato, K., Shichiri, M., and Shiga, K. (1995) Substrate activating mechanism of short-chain acyl-CoA, medium-chain acyl-CoA, long-chain acyl-CoA, and isovaleryl-CoA dehydrogenases from bovine liver: A resonance Raman study on the 3-ketoacyl-CoA complexes. *J. Biochem.* **118**, 900-910
17. Powell, P.J., Lau, S.-M., Killian, D., and Thorpe, C. (1987) Interaction of acyl-coenzyme A substrates and analogues with pig kidney medium-chain acyl-CoA dehydrogenase. *Biochemistry* **26**, 3704-3710
18. Nishimoto, K., Imamura, A., Yamaguchi, K., Yamabe, S., and Kitaura, K. (1989) *Bunshisekkei no tameno Ryoushikagaku* (in Japanese), Kodansha Scientific, Tokyo
19. Nishimoto, K., Fukunaga, H., and Yagi, K. (1986) Studies in a model system on the effect of hydrogen bonding at hetero atoms of oxidized flavin on its electron acceptability. *J. Biochem.* **100**, 1647-1653
20. Sykes, P. (1981) *A Guidebook to Mechanism in Organic Chemistry. Fifth Edition*, p. 274, Longman, London, New York
21. Breitmaier, E. and Voelter, W. (1987) *Carbon-13 NMR Spectroscopy. High-Resolution Methods and Applications in Organic Chemistry and Biochemistry. Third, Completely Revised Edition*, p. 232, VCH, Weinheim, New York
22. Breitmaier, E. and Voelter, W. (1987) *Carbon-13 NMR Spectroscopy. High-Resolution Methods and Applications in Organic Chemistry and Biochemistry. Third, Completely Revised Edition*, p. 111, VCH, Weinheim, New York
23. Johnson, B.D., Mancini-Samuelson, G.J., and Stankovich, M.T. (1995) Effect of transition-state analogues on the redox properties of medium-chain acyl-CoA dehydrogenase. *Biochemistry* **34**, 7047-7055
24. Trievel, R.C., Wang, R., Anderson, V.E., and Thorpe, C. (1995) Role of the carbonyl group in thioester chain length recognition by the medium chain acyl-CoA dehydrogenase. *Biochemistry* **34**, 8597-8605